Supporting Information

S1 Gating Strategies

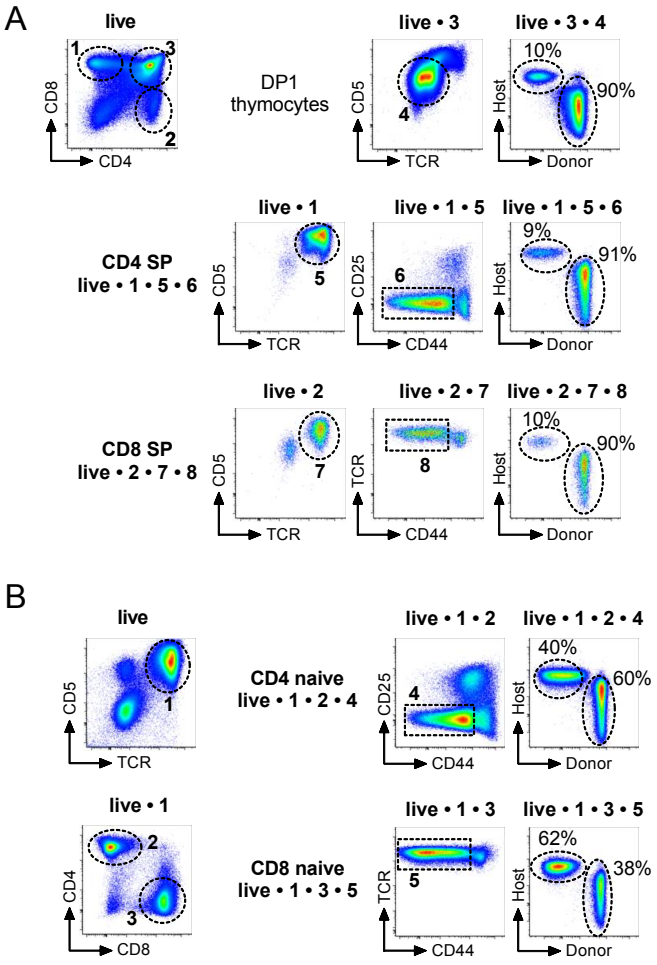

Figure S1.1: **Gating strategy for identification of naive CD4 and CD8 lymphocytes in busulfan chimeras**. (A) Gating thymic subsets. Density plot headings indicate the gates applied to the corresponding plot. Electronic gates are indicated in dashed lines and numbered. CD4 SP were analysed by applying the gate 'live•1•5•6' to identify CD4+CD8-TCR^{hi}CD5^{hi}CD44^{lo} CD25- cells. CD8 SP were analysed by applying 'live•2•7•8' to identify CD4-CD8+TCR^{hi}CD5^{hi}CD44^{lo} cells. (B) Gating lymph node subsets. CD4 naive were analysed by applying 'live•1•2•4' to identify CD4+TCR^{hi}CD5^{hi}CD44^{lo}CD25- cells. CD8 naive were analysed by applying 'live•1•3•5' to identify CD8+TCR^{hi}CD5^{hi}CD44^{lo} cells.

S2 Fitting two datasets simultaneously

Fitting two functions, potentially with common parameters, to two distinct sets of data requires combining two partial likelihoods and we recap the formalism here. Let $f(x)$ and $g(x)$ be the functions we wish to fit to each dataset, and $\mathcal{F} = T_f(f)$ and $\mathcal{G} = T_g(g)$ are transformed functions that for best-fit parameters yield normally distributed residuals. If the two datasets have n_f and n_g observations respectively, the likelihood is

$$\begin{aligned}\mathcal{L} &= \prod_i^{n_f} \frac{1}{\sqrt{2\pi}\sigma_i} \exp\left(\frac{-(x_i - \mathcal{F}_i)^2}{2\sigma_i^2}\right) \times \prod_j^{n_g} \frac{1}{\sqrt{2\pi}\sigma_j} \exp\left(\frac{-(x_j - \mathcal{G}_j)^2}{2\sigma_j^2}\right) \\ &= \frac{\exp\left(-\mathrm{RSS}_\mathcal{F}/2\sigma_\mathcal{F}^2\right)}{\left(\sqrt{2\pi}\sigma_\mathcal{F}\right)^{n_f}} \times \frac{\exp\left(-\mathrm{RSS}_\mathcal{G}/2\sigma_\mathcal{G}^2\right)}{\left(\sqrt{2\pi}\sigma_\mathcal{G}\right)^{n_g}},\end{aligned} \tag{S2.1}$$

where RSS denotes the residual sum of squares and we assume constant and unknown variances $\sigma_\mathcal{F}^2$ and $\sigma_\mathcal{G}^2$ within each set of observations. The log-likelihood is then

$$\ln\mathcal{L} = -n_f \ln\left(\sqrt{2\pi}\sigma_\mathcal{F}\right) - n_g \ln\left(\sqrt{2\pi}\sigma_\mathcal{G}\right) - \frac{\mathrm{RSS}_\mathcal{F}}{2\sigma_\mathcal{F}^2} - \frac{\mathrm{RSS}_\mathcal{G}}{2\sigma_\mathcal{G}^2}. \tag{S2.2}$$

Maximum likelihood estimates of $\sigma_\mathcal{F}^2$ and $\sigma_\mathcal{G}^2$ are given by

$$\partial_{\sigma_k}\mathcal{L} = -\frac{n_k}{\sigma_k} + \frac{\mathrm{RSS}_k}{\sigma_k^3} = 0 \implies \hat{\sigma}_k^2 = \frac{\mathrm{RSS}_k}{n_k}.$$

Substituting these into equation S2.2 gives the following expression for the combined log-likelihood,

$$\ln\mathcal{L} = -\frac{1}{2}\ln\left[\left(\mathrm{RSS}_\mathcal{F}^{n_f}\right)\left(\mathrm{RSS}_\mathcal{G}^{n_g}\right)\right] - (n_f + n_g). \tag{S2.3}$$

In the case $n_f = n_g = n$, which applies to all datasets considered in this study, the quantity to maximise is the sum of the log likelihoods or, equivalently, minimising the product of the residual sum of squares within each dataset:

$$\ln\mathcal{L} = -\frac{n}{2}\ln\left(\mathrm{RSS}_\mathcal{F} \times \mathrm{RSS}_\mathcal{G}\right) - 2n. \tag{S2.4}$$

When quoting AIC values, we use the sample-size-corrected expression

$$\mathrm{AIC_c} = n\ln\left(\mathrm{RSS}_\mathcal{F} \times \mathrm{RSS}_\mathcal{G}\right) + 2k + \frac{2k(1+k)}{2n-k-1}, \tag{S2.5}$$

which is correct up to terms in the log likelihood containing n only, and the number of observations is $2n$.

S3 Comparison of rescaled donor fractions normalised to DP1 and SP

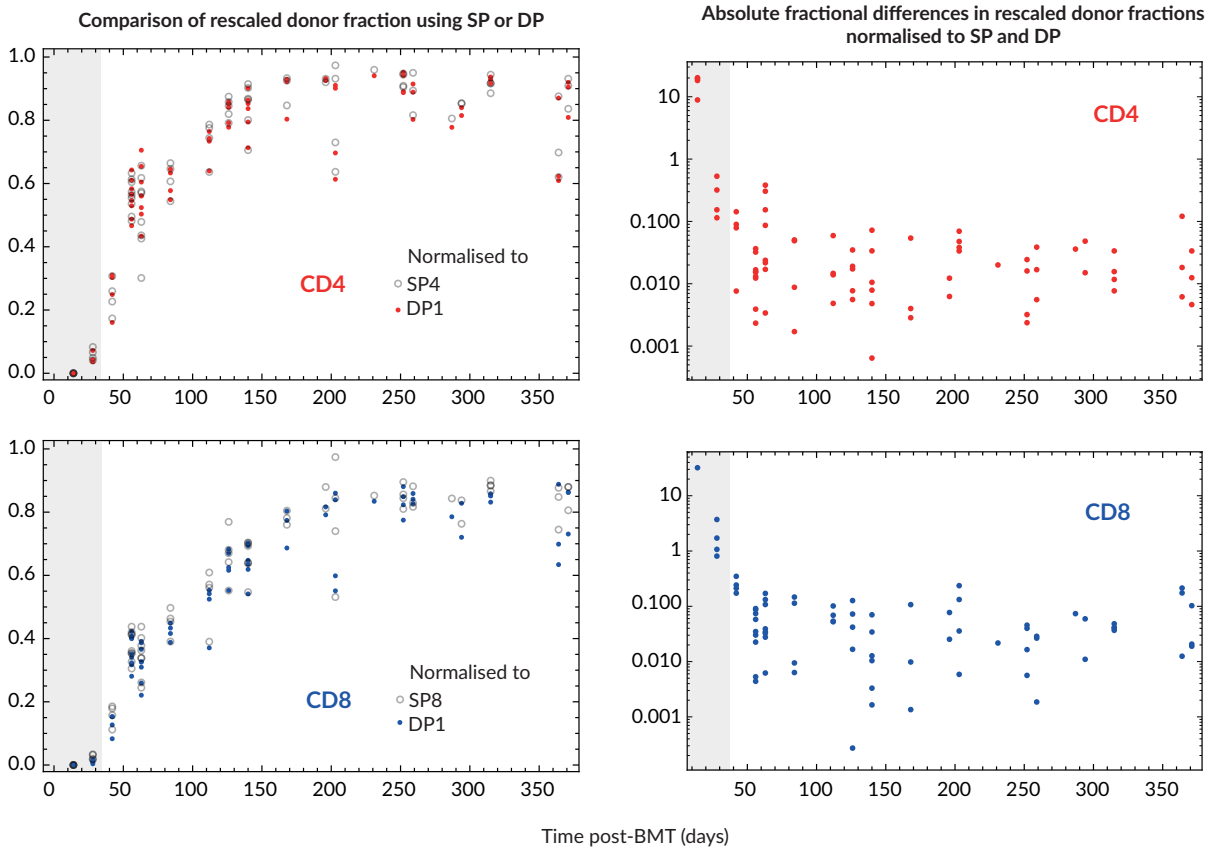

Figure S3.1: Comparing the timecourses of the donor fraction in the periphery normalised to the relevant single-positive (SP) population (open circles, as used in the analyses) and DP1 (solid circles). Shaded regions contain data obtained before equilibration of the donor fraction at all developmental stages in the thymus (taken to be complete at 42 days post-BMT) and were not used for fitting (see main text).

S4 Very general homogeneous models cannot explain kinetics of peripheral chimerism

The simplest model of naive population dynamics with constant rates of division and death was unable to explain the normalised donor fraction asymptoting to a value less than 1, suggesting the model of incumbents and displaceable cells. Here we explore the possibility that a kinetically homogeneous population with time-varying rates of divison and death can explain the data. This model is

$$\begin{aligned}\frac{\mathrm{d}N(t)}{\mathrm{d}t} &= \theta(t) - [\delta(t) - \rho(t)]\, N(t), \\ &= \Theta e^{-\nu t} - \lambda(t) N(t),\end{aligned} \tag{S4.1}$$

where thymic involution occurs exponentially (Figure 2 in the main text). We take $\lambda(t) = \delta(t) - \rho(t) \geq 0$ since total cell counts are decreasing for part of the timecourse; were $\lambda(t)$ to be negative, $dN(t)/dt$ would be greater than zero $\forall t$.

Using this fact to define $\Lambda(t) = \int_0^t \lambda(t')dt' \geq 0$, and following the previous logic, we can define a pair of such equations, one each for donor and host populations, and calculate the donor fraction. This yields

$$f_d(t) = 1 - \frac{1 - f_d(0)}{1 + \frac{\Theta}{N_0}\int_0^t e^{-\nu t' + \Lambda(t')} dt'} \tag{S4.2}$$

where we have made use of $\exp[\Lambda(0)] = 1$. If the integral in the above expression diverges, then $f_d \to 1$ regardless of the other parameters. Here it is sufficient to consider the situation in which the integral converges as fast as possible, and show that this is still too slow to describe the observed data.

Because $\Lambda(t)$ is a positive non-decreasing function, the integrand will decrease fastest when $\Lambda(t)$ is a small constant. In this case, the integral can be solved analytically as

$$\begin{aligned}\int_\tau^{t>\tau} e^{-\nu t' + \Lambda(t')} dt' &\simeq \int_\tau^{t>\tau} e^{-\nu t' + \Lambda_{\max}} dt', \\ &= \frac{e^{\Lambda_{max}}}{\nu}\left(e^{-\nu\tau} - e^{-\nu t}\right).\end{aligned} \tag{S4.3}$$

where $t = \tau \geq 0$ corresponds to the point at which the integrand has a maximum. Thus the integral converges according to the exponential time constant ν which is relatively slow. Even if the integral were to begin converging from the start of the timecourse, with $\nu \sim 0.0048$ days^{-1} it would only have converged to within 5% by approximately 600 days, well beyond what is observed.

Therefore using estimates of ν we have shown that using a fairly general $\lambda(t)$ one cannot simultaneously satisfy the requirement that the total cell counts be decreasing at large t, and have the donor fraction asymptote in the time frame observed.

S5 Fitting the incumbent-displaceable model

We extended the model to include a population of host cells resistant to displacement ('incumbents'). The model is described in equations 8-10 in the main text. Solving these equations with initial conditions $N_h(0) = N_0 - N_d(0)$, $I_h(0) = I_0$ and $N_d(0) = \chi f_d(0)(N_0 + I_0)$ gives

$$\begin{aligned} \text{Normalised donor fraction } f_d &= \frac{N_d(t)}{N_h(t) + I_h(t) + N_d(t)} / \chi, \\ &= \frac{\left(e^{(\lambda-\nu)t} - 1\right) \Theta/N_0 + (1 + I_0/N_0)\,(\lambda - \nu) f_d(0)}{(\lambda - \nu)\left[(I_0/N_0)e^{(\lambda-\lambda_I)t} + 1\right] + (\Theta/N_0)\left[e^{(\lambda-\nu)t} - 1\right]}, \end{aligned} \tag{S5.1}$$

where here $t = 0$ corresponds to the time at which host:donor chimerism has stabilised at all stages of thymic development, and not the time of treatment.

The population sizes I_0 and N_0 and the rate of thymic output Θ will vary across animals. However we expect the ratios I_0/N_0 and N_0/Θ to be only weakly dependent on chimerism and body mass since, as before, thymic output might reasonably be assumed proportional to the sizes of peripheral naive populations. Hence we took equation S5.1 to be applicable across animals. Fitting it to the normalised donor fraction alone potentially allowed cell counts to reach unphysiological values, so to avoid this we fitted simultaneously to the normalised donor fraction (equation S5.1) and the total naive cell counts, yielding estimates for λ, λ_I, I_0, N_0, Θ, and $f_d(0)$.

S6 Naive phenotype is preserved in host and donor cells over a year post-treatment

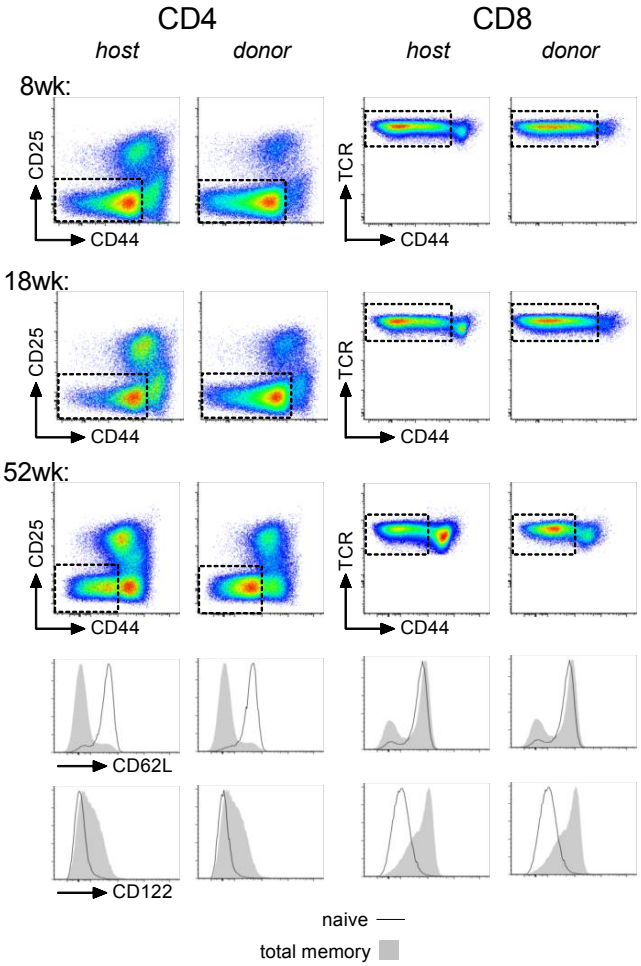

Figure S6.1: **Donor and host naive T cell phenotype in busulfan chimeras**. Busulfan chimeras were generated using CD45.1 hosts reconstituted with CD45.2 donor bonemarrow (see Methods). Density plots show CD25 vs CD44 by CD4+TCR^{hi}CD5^{hi} T cells amongst CD45.1 host or CD45.2 donor origin populations, and CD44 vs TCR by CD8+TCR^{hi}CD5^{hi} T cells amongst CD45.1 host or CD45.2 donor origin populations. Boxes indicate gates used to identify naive T cells. Data shown from chimeras 8 wks, 18 wks and 52 wks after reconstitution. Histograms show CD62L and CD122 expression by naive gated CD4 (columns 1-2) and CD8 (columns 3-4) T cells of host origin (columns 1,3) and donor origin (columns 2,4) (thin black lines), compared with total CD44^{hi}CD25- memory populations of the corresponding subset, from the 52wk timepoint.

S7 A model of cell-age-dependent kinetics

Rather than considering the loss rate to be a function of host age, $\lambda(t)$, we can consider $\lambda(a)$ where a denotes the time since a particular cell lineage has left the thymus – that is a is the post-thymic age of a cell and which is assumed to be inherited by daughter cells during division. We postulate that a net loss rate declining with cell age may give rise to the donor fraction profile we see, without needing to invoke a clear distinction between incumbents and displaceable cells. In this case the system is described by the following PDE:

$$\partial_t N(t,a) + \partial_a N(t,a) = -\lambda(a) N(t,a), \tag{S7.1}$$

where $N(t,a)$ is a cell density. The naive T cell population size is $N(t) = \int N(t,a)da$ where we integrate over all allowable cell ages. This can be re-written as

$$\begin{aligned} \frac{dN(t,a)}{dt} &= \partial_t N(t,a) + \partial_a N(t,a)\frac{da}{dt}, \\ &= \partial_t N(t,a) + \partial_a N(t,a), \\ &= -\lambda(a) N(t,a), \end{aligned} \tag{S7.2}$$

using $da/dt = 1$. The boundary conditions of this problem are

$$\begin{aligned} N(0,a) &= g(a), \\ N(t,0) &= \theta(t), \end{aligned} \tag{S7.3}$$

where $g(a)$ is the initial age distribution of cells and $\theta(t)$ is the rate of thymic output, *i.e.* cells with age $a = 0$. Here we outline the general procedure for solving this system, and then further subdivide into host and donor compartments.

We approach this by treating separately the cells present in the periphery at time $t = 0$, $N_{\text{init}}(t,a)$, and those generated subsequently by the thymus, $N_\theta(t,a)$. We deal with pre-existing cells first. Because $da/dt = 1$, $t = a - s$ for some constant s and we can re-write eqn. S7.2 and its boundary condition as

$$\begin{aligned} \frac{d}{dt} N_{\text{init}}(t,s) &= -\lambda(t+s) N_{\text{init}}(t,s), \\ N_{\text{init}}(0,s) &= g(s). \end{aligned} \tag{S7.4}$$

This is an implementation of the method of characteristics which tracks the fate of a cohort of cells of initial ages in the range $(s, s+ds)$, drawn from some initial age distribution $g(s)$, from time $t = 0$ and subject to the age-dependent loss rate $\lambda(a) = \lambda(t+s)$. The parameter s thus indexes the cohorts and can be considered a constant. $N_{\text{init}}(t,s)$ is the density of cells in the periphery at time t deriving from the cells of age s at $t = 0$,

$$N_{\text{init}}(t,s) = g(s) \exp\left(-\int_0^t \lambda(\tau + s) d\tau \right). \tag{S7.5}$$

obtained by solving (S7.4). This gives

$$N_{\text{init}}(t,a) = g(a-t) \exp\left(-\int_0^t \lambda(\tau + a - t) d\tau \right), \quad \text{for } a \geq t. \tag{S7.6}$$

To this population we add all surviving cells that emerged from the thymus from $t = 0$ onwards. The number of such 'new' cells of age a at time t, $N_\theta(t,a)$, is governed by the same equation but with a different boundary condition:

$$\begin{aligned} \frac{dN_\theta(t,a)}{da} = \partial_a N_\theta(t,a) + \partial_t N_\theta(t,a)\frac{dt}{da} &= -\lambda(a) N_\theta(t,a), \\ N_\theta(t,0) &= \theta(t). \end{aligned}$$

Using $t = a + s$ for some constant s,

$$\begin{aligned} \frac{d}{ds} N_\theta(s,a) &= -\lambda(a) N_\theta(s,a), \\ N_\theta(s,0) &= \theta(s), \\ \implies N_\theta(s,a) &= \theta(s) \exp\left(-\int_0^a \lambda(\tau) d\tau \right), \end{aligned}$$

which gives

$$N_\theta(t,a) = \theta(t-a) \exp\left(-\int_0^a \lambda(\tau) d\tau \right) \quad \text{for } a \leq t. \tag{S7.7}$$

The total density of cells of age a at time t, $N(t,a)$, is therefore the sum of the two population densities (S7.6) and (S7.7). The thymus is the source of the initial distribution of cells, which gives us the continuity condition $N_\theta(0,0) = N_{\text{init}}(0,0)$, or $g(0) = \theta(0)$.

To apply the above formalism to busulfan chimeras, first we define $t = 0$ to be the time of bone marrow transplant (BMT). This definition is in contrast to the incumbent/displaceable model, in which time is measured from the point that the host/donor composition of the thymus has equilibrated. The age distribution of donor cells at BMT is therefore zero ($g_d(a) = 0$). We then have three functions to consider: the initial host population $N^h_{\text{init}}(t,a)$, host cells exported post-BMT $N^h_\theta(t,a)$, and donor cells $N^d_\theta(t,a)$.

To connect to the observations, we integrate over cell age a to give the host and donor population sizes $N_h(t)$ and $N_d(t)$, from which we obtain the total naive T cell population size and the normalised donor fraction f_d. We also need to specify the rates of thymic output $\theta_h(t)$ and $\theta_d(t)$; the loss rate $\lambda(a)$; and the age distribution of host cells at BMT, $g(a)$. We assume that total thymic export $\theta_{\text{total}}(t) = \theta_{\text{total}}(0)e^{-\nu t}$, where ν is the rate of thymic involution and $t = 0$ is the time of BMT, and that total thymic export is unaffected by treatment (Figure 1D). Following BMT, donor cell output reaches its saturating level $\chi\theta_{\text{total}}(t)$ over a timescale τ and host cell output falls in tandem to $(1-\chi)\theta_{\text{total}}(t)$. We assume that the net rate of loss in the periphery $\lambda(a)$ falls exponentially with time since thymic export at a rate r. The age distribution of host cells at $t = 0$ is unknown; we assumed an increasing, power-law dependence of g on a, over-representing older cells, corresponding to cells exported soon after birth proliferating more than those exported later. With these constraints and assumptions we then have:

$$\begin{aligned}
\theta_d(t) &= \theta_{\text{total}}\chi \begin{cases} (t/\tau)^{1/\mu} & : t \le \tau \\ 1 & : t > \tau \end{cases} \\
\theta_h(t) &= \theta_{\text{total}} - \theta_d(t), \\
\lambda(a) &= \ell e^{-ra}, \\
g(a) &= \begin{cases} Aa^p + \theta_h(0) & : a \le a_{\text{BMT}} \\ 0 & : a > a_{\text{BMT}} \end{cases}
\end{aligned} \tag{S7.8}$$

where the parameter μ controls the steepness of the transition to stable chimerism and a_{BMT} is the mouse age at treatment (typically 8 weeks). The constant A is determined by the condition $\int_0^{a_{\text{BMT}}} g(a)da = N_0$, where N_0 is the peripheral population size at treatment. Allowing N_0 to be a free parameter resulted in unphysiological values, and so we set this to 2.78×10^7 and 2.13×10^7 for CD4 and CD8 respectively, based on counts in busulfan chimeras mice at that age. The form chosen for $g(a)$ automatically satisfies the continuity condition $g(0) = \theta(0) = \theta_h(0)$.

We fitted this model to the data for three values of $p \in \{1/2, 1, 2\}$. We found clear support for $p = 1/2$ for CD4 T cells but equal support for all values of p for CD8 cells (Table S7.1). The form of $\lambda(a)$ above represents the case where cells' competitive fitness increases continuously with age; we also investigated unimodal forms for λ, giving competitive advantages to both very young and older cells, but these yielded inferior fits (Table S7.1). Fits to CD4 and CD8 data using $p = 1/2$, and selected parameter estimates, are shown in Figure S7.1; details of parameter estimates are in Table S7.2; values are consistent with those predicted by the incumbent/displaceable model.

	p	$\lambda(a) = \ell e^{-ra}$	$\lambda(a) = a\ell e^{-ra}$	$\lambda(a) = (a+k)\ell e^{-ra}$
ΔAIC_4	1/2	**0**	8.28	2.08
	1	1.14	8.38	3.28
	2	3.27	8.52	4.47
ΔAIC_8	1/2	**0.035**	14.07	2.15
	1	**0.019**	13.94	2.14
	2	**0**	13.79	15.39
Number of fitted parameters (including Θ_0)	-	3	3	4

Table S7.1: **Comparison of age-structured models**. AIC differences for different functional forms of the cell-age-dependent loss rate $\lambda(a)$ and initial age-distribution of mature naive cells, $g(a)$.

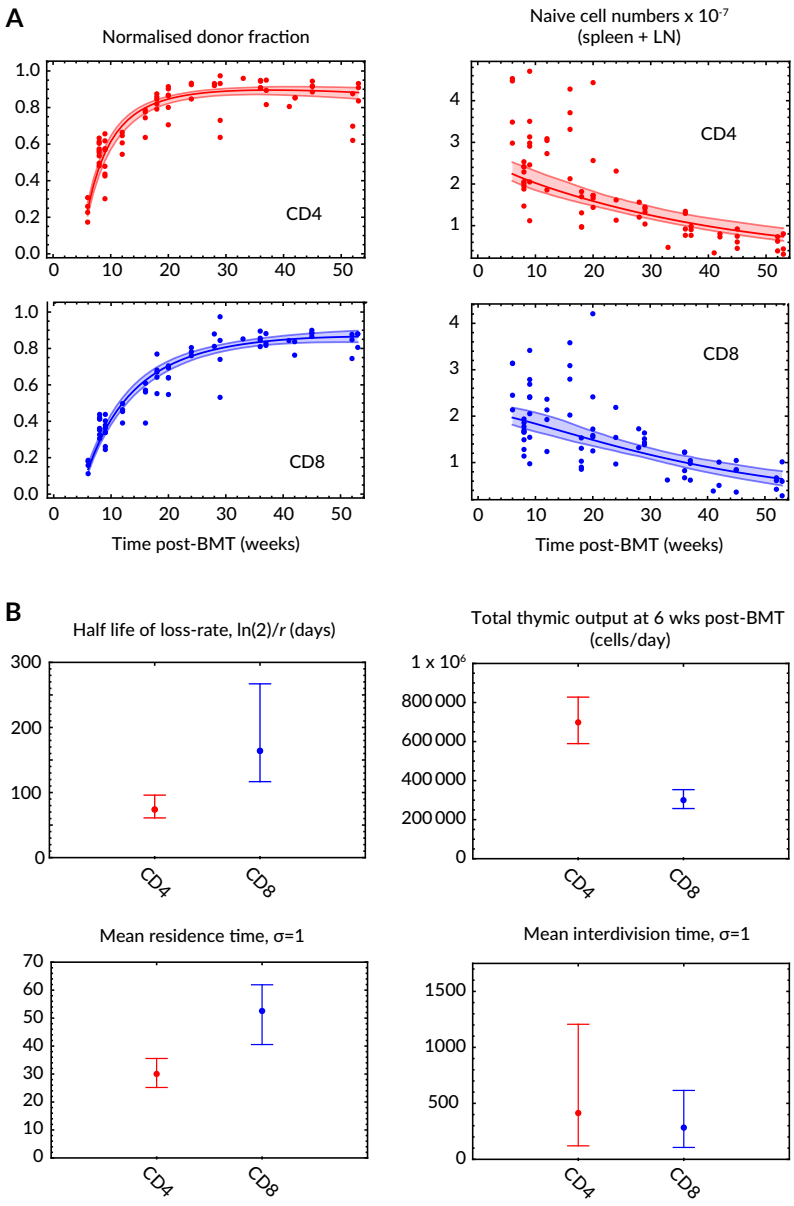

Figure S7.1: **The age-dependent turnover model.** **A** Normalised donor fractions and total naive counts, plus fits. Shaded regions represent 95% confidence envelopes. **B** Parameter estimates in days (see Table S7.2 for numerical values).

	Parameter	Relative loss rate Ki67$^{\mathrm{hi}}$ /Ki67$^{\mathrm{lo}}$	Naive CD4	Naive CD8
Mean net-loss rate (/day)	$\bar{\lambda}$	–	$0.031\ (0.026, 0.035)$	$0.015\ (0.013, 0.017)$
Half-life of function (days)	$\ln(2)/r$	–	$74\ (61, 96)$	$164\ (117, 267)$
Net loss rate of new cells (RTE) (/day)	$\lambda(0) = \ell$	–	$0.047\ (0.037, 0.054)$	$0.021\ (0.017, 0.026)$
Daily thymic output at 6 weeks post-BMT	$\theta_{\mathrm{total}}(42)$	–	$6.98\ (5.89, 8.27) \times 10^5$	$2.99\ (2.57, 3.52) \times 10^5$
Daily thymic output as proportion of peripheral numbers 6 weeks post-BMT	$\theta_{\mathrm{total}}(42)/N(42)$	–	$0.031\ (0.026, 0.036)$	$0.015\ (0.013, 0.018)$
Expected residence time (days)	$1/\delta$	**1**	$30\ (25, 35)$	$53\ (41, 62)$
Expected interdivision time (days)	$1/\rho$	**1**	$408\ (121, 1190)$	$283\ (106, 615)$

Table S7.2: **Kinetic parameter estimates using the age-structured model of heterogeneity.** $\bar{\lambda}$ is the value averaged over the best-fit distribution of cell ages $N(t, a)$, and the residence and interdivision times are mouse-lifetime averages, using $\bar{\lambda}$ with the measured Ki67 expression levels (Figure 4 in main text) and the procedure described in Supporting Information S8.

S8 Using Ki67 expression to extract division and death rates from the net loss rate

Figure S8.1 illustrates an extension to the basic model of homogeneous turnover that distinguishes between cells that are quiescent, Ki67$^{\rm lo}(X)$, and those that are dividing or recently divided, Ki67$^{\rm hi}(Y)$. The return to from high to low Ki67 expression takes place at a rate β;

$$\frac{\mathrm{d}X}{\mathrm{d}t} = \theta(t)(1-\epsilon) + \beta Y(t) - (\alpha + \delta_X)X(t) \tag{S8.1}$$

$$\frac{\mathrm{d}Y}{\mathrm{d}t} = \theta(t)\epsilon + \alpha\left[2X(t) + Y(t)\right] - (\beta + \delta_Y)Y(t) \tag{S8.2}$$

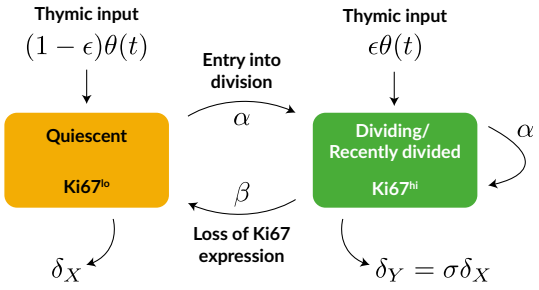

Figure S8.1: Simple two-compartment model of homeostatic proliferation using Ki67 as a marker of dividing and recently divided cells.

The parameter ϵ is the proportion of cells leaving the thymus that are Ki67$^{\rm hi}$ as they enter the naive pool. Recalling equation 1 in the main text,

$$\frac{\mathrm{d}N}{\mathrm{d}t} = \theta(t) + (\rho - \delta)\,N(t),$$

the proliferation rate ρ is then calculated by equating the total rate of non-thymic production of cells in the single-compartment model and the extended model in Figure S8.1. Adding Eqns. S8.1 and S8.2 gives

$$\frac{\mathrm{d}(X+Y)}{\mathrm{d}t} \equiv \frac{\mathrm{d}N}{\mathrm{d}t} = \theta(t) + \alpha(X+Y) - (\delta_X X + \delta_Y Y)$$

giving $\rho N = \alpha(X+Y)$ and $\delta N = \delta_X X + \delta_Y Y$. We assume thymic output $\theta(t)$ changes slowly relative to the rate of return to Ki67$^{\rm lo}$ from Ki67$^{\rm hi}$, and so X and Y are in quasi-equilibrium. If κ is the measured fraction of cells that are Ki67$^{\rm hi}$, $Y/(X+Y)$, then

$$\rho = \alpha, \qquad \kappa = \frac{\alpha(2-\epsilon) + \delta_X\epsilon}{\alpha + \beta + \delta_Y + \epsilon(\delta_X - \delta_Y)}$$

which after eliminating α gives

$$\rho = \frac{\delta_Y\kappa(1-\epsilon) + \kappa\beta - \delta_X\epsilon(1-\kappa)}{2 - \kappa - \epsilon} \tag{S8.3}$$

Similarly, if σ is the relative susceptibilty to death of Ki67$^{\rm hi}$ over Ki67$^{\rm lo}$ cells, such that $\delta_Y = \sigma\delta_X$, then

$$\delta = \delta_Y\left(\frac{1-\kappa}{\sigma} + \kappa\right). \tag{S8.4}$$

Using Eqns. S8.3 and S8.4 with the relation $\lambda = \delta - \rho$ we obtain the proliferation rate as a function of measurable parameters – the net loss rate in the periphery λ, the Ki67$^{\rm hi}$ fraction κ, the mean lifetime of Ki67 expression, $T = 1/\beta$, and σ;

$$\rho = \frac{\kappa(1 + \kappa(\sigma-1) + \lambda T(\epsilon + \sigma - \epsilon\sigma)) - \lambda T\epsilon}{T(1-\kappa)(2 + \kappa(\sigma-1))}, \quad \delta = \lambda + \rho = \frac{(1 + \kappa(\sigma-1))(\kappa + \lambda T(2 - \epsilon - \kappa))}{T(1-\kappa)(2 + \kappa(\sigma-1)}. \tag{S8.5}$$

In all results presented in the main text we assumed $\epsilon = 0.2$ but Figure S8.2 depicts the mean residence time as a function of both ϵ and σ. For the value of ϵ used in our primary calculations there is no unphysical region, as depicted in Figure S8.2, for either cell type.

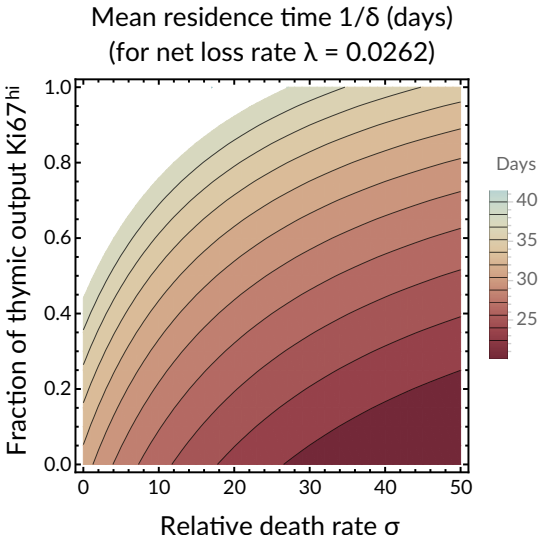

Figure S8.2: **Effect of the level of Ki-67 expression in cells leaving the thymus on the estimated mean residence times of naive CD4 T cells**. Here we plot $1/\delta$ as in equation S8.4 using the best-fit value of the net loss rate, $\lambda = 0.0262$/day and the mean Ki67$^{\rm hi}$ fraction $\kappa = 0.045$; and $T = 1/\beta = 4$ days. The area beyond the dashed line represents an unphysical region where $\rho < 0$. Shown for parameters estimated from CD4 cells. For CD8 cells, $\lambda \simeq 0.0143$/day and the unphysical region is vanishingly small.

S9 A homogeneous model with declining efficiency of RTE incorporation

Here we consider another alternative to the incumbent model in which we aim to explain the incomplete replacement with donor cells by assuming that the rate at which RTE mature into naive cells declines with the age of the host. We assume that host and donor cells are kinetically identical, and partition RTE kinetics into the difference between division and death, λ_r, which we assume is constant with age, and a declining rate of differentiation into mature naive cells, $\mu\exp(-kt)$. Four ODEs describe this system – for RTE,

$$\begin{aligned} R_d'(t) &= \chi\Theta e^{-\nu t} - (\mu e^{-kt} + \lambda_r)R_d(t), \\ R_h'(t) &= (1-\chi)\Theta e^{-\nu t} - (\mu e^{-kt} + \lambda_r)R_h(t), \end{aligned} \tag{S9.1}$$

and for mature naive cells,

$$\begin{aligned} N_d'(t) &= \mu e^{-kt}R_d(t) - \lambda N_d(t), \\ N_h'(t) &= \mu e^{-kt}R_h(t) - \lambda N_h(t). \end{aligned} \tag{S9.2}$$

Thymic export $\Theta\exp(-\nu t)$ and chimerism χ are defined as before. We required two new initial conditions, $R_d(0)$ and $R_h(0)$. As before we assume the initial donor counts are proportional to the level of chimerism, χ, giving $R_d(0) = \chi\beta_R R_0$ and $N_d(0) = \chi\beta_N N_0$ where $R_0 = R_d(0) + R_h(0)$ and similarly for N_0. This mapping of the initial conditions to the common parameters $\beta_{(.)}$ makes the rescaled donor fraction independent of χ as required for a global fit.

Equations S9.1 and S9.2 were solved numerically and used to construct the total count and rescaled donor fraction functions. Coupled with the minimization procedure outlined in Section S5 we fit this model to the data (Figure S9.1, solid lines). It describes the data comparably to the incumbent model (dashed lines), but the latter has significantly more statistical support by virtue of having 5 parameters instead of 9 ($\Delta\text{AIC}_4 = 8.45$, $\Delta\text{AIC}_8 = 8.75$).

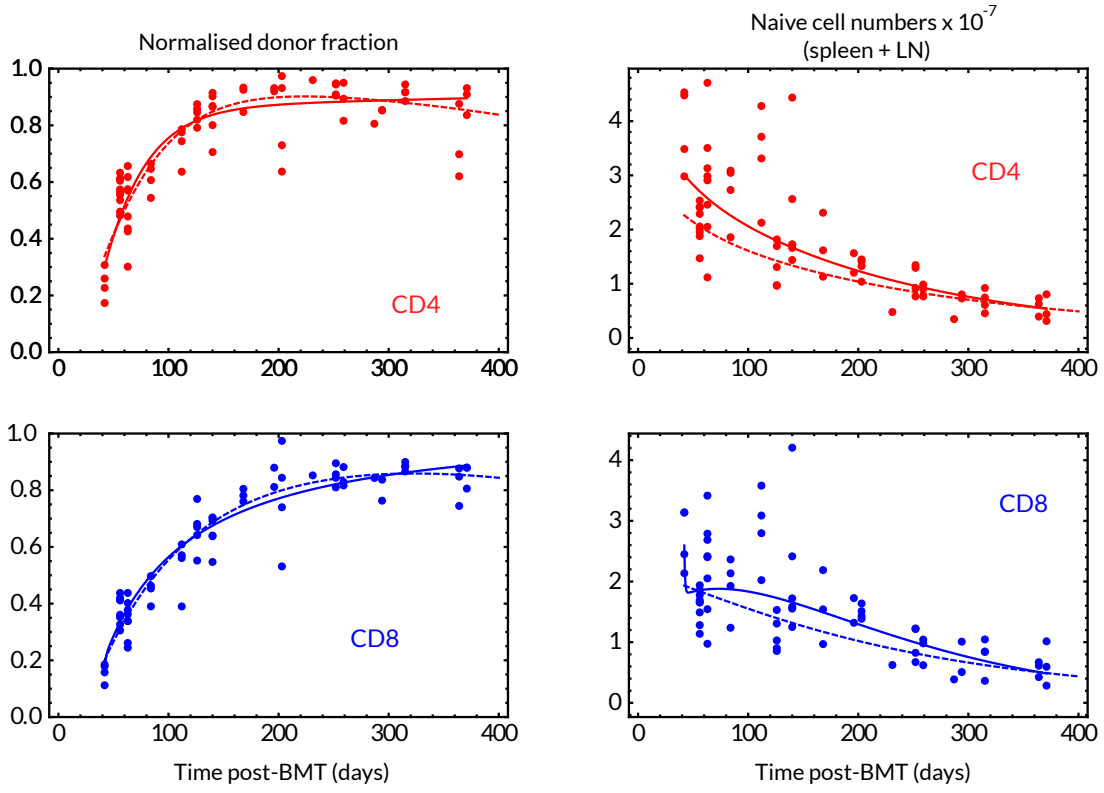

Figure S9.1: **Comparison of the incumbent and RTE models**. Normalized donor fractions and total naive counts with RTE model (solid line) and incumbent model (dashed line) fits.